Organic LETTERS

Letter

pubs.acs.org/OrgLett

Synthesis of Boron-Doped Polycyclic Aromatic Hydrocarbons by Tandem Intramolecular Electrophilic Arene Borylation

Fumiya Miyamoto,[†] Soichiro Nakatsuka,[†] Keitaro Yamada,[‡] Ken-ichi Nakayama,*[,‡] and Takuji Hatakeyama*[,†,§]

[†]School of Science and Technology, Kwansei Gakuin University, Gakuen 2-1, Sanda, Hyogo 669-1337, Japan

[‡]Graduate School of Science and Engineering, Yamagata University, 4-3-16, Jonan, Yonezawa, Yamagata 992-8510, Japan

[§]Elements Strategy Initiative for Catalysts and Batteries, Kyoto University, Katsura, Kyoto 615-8520, Japan

Supporting Information

ABSTRACT: Tandem intramolecular electrophilic arene borylation was developed to facilitate access to B-doped polycyclic aromatic hydrocarbons (PAHs). DFT calculations revealed that electrophilic arene borylation occurred via a four-membered ring transition state, in which C−B and H−Br bonds formed in a concerted manner. An organic light-emitting diode employing the B-doped PAH as an emitter and a B-doped PAH-based field-effect transistor were successfully fabricated, demonstrating the potential of B-doped PAHs in materials science.

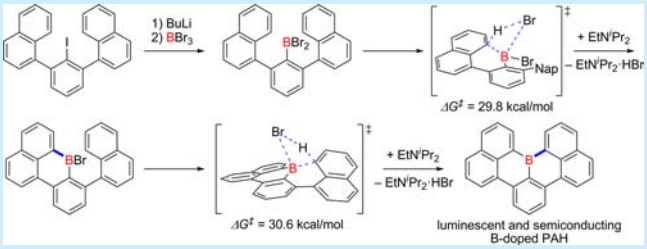

Heteroatom-doped graphene is one of the most attractive materials for a field-effect transistor (FET), an anode in Li-ion batteries, and a cathode catalyst in fuel cells.[1,2] A promising method for producing it is by chemical doping of heteroatoms into graphene.[1] Another promising method is chemical vapor deposition, which has been applied for the synthesis of nitrogen-doped graphene.[2] However, typically, complex mixtures have been obtained by these approaches, and the effect of doping on physical properties has not been elucidated in detail. For these reasons, it is desirable to develop a bottom-up synthesis based on the surface-assisted coupling[3] or amplification sheet growth[4] of heteroatom-doped polycyclic aromatic hydrocarbons (PAHs),[5] which is potentially advantageous for the production of well-defined heteroatom-doped graphene.

Recently, B-doped PAHs have attracted significant attention not only as a starting unit for bottom-up synthesis but also as a well-defined substructure for B-doped graphene. Yamaguchi and co-workers have synthesized B-doped PAHs by dehydrogenative aromatic C−C coupling and have reported their remarkable chemical and thermal stabilities.[5d,e] However, from the materials science viewpoint, it is desirable to establish a robust, scalable reaction for constructing B-doped PAH frameworks. Herein, a novel, facile approach based on tandem intramolecular electrophilic arene borylation is reported[6] (Scheme 1). The reaction developed herein is simple and affords products in high yield, thereby facilitating gram-scale synthesis of B-doped PAHs. The mechanistic details are elucidated by density functional theory (DFT) calculations. Moreover, an organic light-emitting diode (OLED)[7] employing the B-doped PAH as an emitter and a B-doped PAH-based FET[8] are fabricated to demonstrate its promising potential in materials science.

Scheme 1. Tandem Intramolecular Electrophilic Arene Borylation toward B-Doped Polycyclic Aromatic Hydrocarbons (PAHs)

Scheme 2 shows the synthetic route: The 2 position of 1,3-dichlorobenzene underwent selective lithiation, followed by

Scheme 2. Synthesis of B-Doped PAH 3

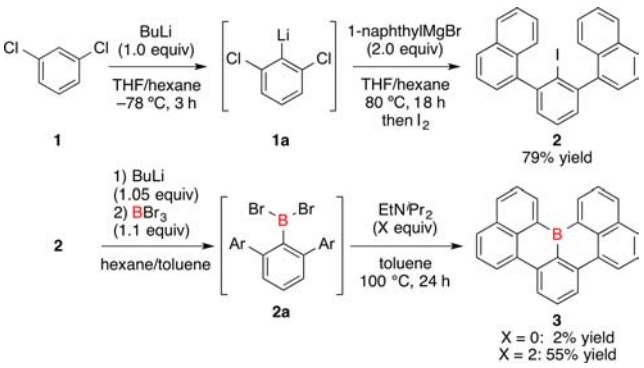

Received: November 2, 2015
Published: November 25, 2015

DOI: 10.1021/acs.orglett.5b03167
Org. Lett. 2015, 17, 6158−6161

treatment with 2 equiv of 1-naphthylmagnesium bromide, to afford *m*-teraryl iodide **2** in 79% yield by quenching with iodine.[9] Next, **2** was subjected to lithium−halogen exchange, followed by the trapping of the resulting aryllithium with boron tribromide, to afford *m*-terarylboron dibromide **2a**. Next, the additives and reaction conditions were carefully screened; the tandem intramolecular electrophilic arene borylation of **2** was achieved at 100 °C in the presence of 2 equiv of EtN^iPr_2 to afford B-doped PAH **3** in 55% yield. In the absence of EtN^iPr_2, the product was obtained in 2% yield, indicating the reversibility of the current reaction. Notably, synthesis of **3** by nickel(0)-mediated Yamamoto C−C coupling was reported by Wagner et al. very recently.[10] Compound **3** was prepared in three steps from (2,6-dibromophenyl)dimethylboronate using 1-bromo-8-iodonaphthalene as a coupling partner. Although the overall yield of the present two-step protocol (43% yield) is comparable to that of the three-step protocol reported by Wagner et al. (42% yield), the commercial availability of 1,3-dichlorobenzene and 1-naphthylmagnesium bromide is a marked advantage for large-scale production.

As shown in Scheme 3, the versatility of the current reaction was demonstrated by the synthesis of B-doped PAH derivatives

Scheme 3. Synthesis of B-Doped PAH 4

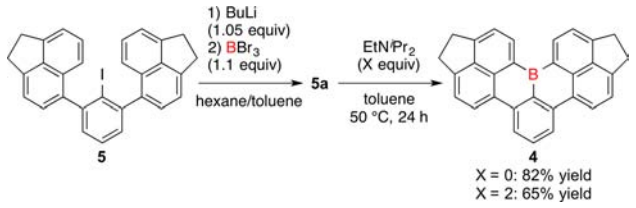

4. In the presence of 2 equiv of EtN^iPr_2, the tandem intramolecular electrophilic arene borylation of *m*-terarylboron dibromide **5a**, prepared from **5**, occurred at 50 °C to afford B-doped PAH **4** in 65% yield. As **4** was practically insoluble in toluene, it was observed as an orange precipitate in the reaction vessel. Interestingly, the reaction smoothly occurred in the absence of EtN^iPr_2 to afford **4** in 82% yield. It is hypothesized that the formation of the precipitate changed the equilibrium of borylation.

To obtain detailed insight into the reaction mechanism, DFT calculations, by the use of the B3LYP-D hybrid functional with the 6-311+G(d,p) basis set, were performed to locate energetically reasonable reaction coordinates starting from **2a** (Figure 1). The first cyclization occurred via **TS1** with an activation energy of 29.8 kcal/mol (ΔG). Interestingly, **TS1** contained a σ-bond metathesis-like four-membered structure, in which C−B bond formation and C−H bond cleavage occurred in a concerted manner. The resulting **INT1** containing HBr was 1.1 kcal/mol less stable than the starting precursor **2a**. Then, HBr was successfully trapped with EtN^iPr_2 in a highly exothermic process, to afford **INT2**. The second cyclization from **INT2** to target compound **3** was very similar to the first cyclization. The activation energy was slightly higher (30.6 kcal/mol), probably because of the less electrophilic nature of the boron center embedded in the π-conjugated framework. The second cyclization was also reversible but was completed with the exothermic trapping of HBr with EtN^iPr_2, which is in good agreement with the experimental results.

Figure 2 shows the X-ray crystallographic structures of **3**. The results were almost identical to those observed in the previous

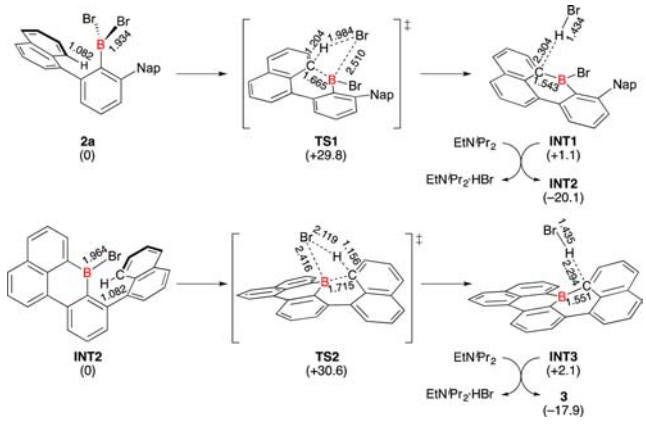

Figure 1. Reaction pathway for electrophilic arene borylation calculated at the B3LYP-D/6-311+G(d,p) level in the presence of toluene by placing the solute in a cavity within the solvent reaction field. Gibbs free energies (kcal/mol) relative to **2a** (above) or **INT2** (below) are shown in parentheses.

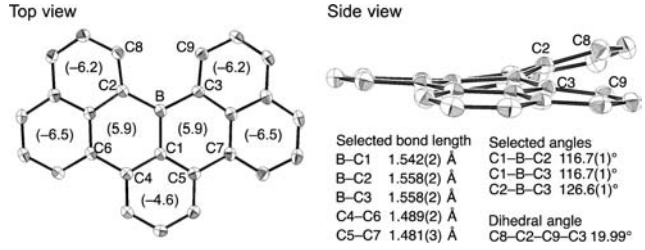

Figure 2. ORTEP drawings of **3**. Thermal ellipsoids are shown at 50% probability; hydrogen atoms are omitted for clarity. NICS(0) values are shown in parentheses.

study.[10] The boron center adopted trigonal planar geometry with three C−B−C bond angles of 116.7(1)°, 116.7(1)°, and 126.6(1)°, respectively (total: 360.0°). Because of the steric repulsion between the hydrogen atoms at the β-position of the boron atom, **3** adopted a helical structure. Although **3** exhibited a nonplanar structure, it was stable toward oxygen, 1 N HCl, and 1 N NaOH. Moreover, decomposition was not observed even at the melting point (174 °C). The three C−B bond lengths were 1.542(2), 1.558(2), and 1.558(2) Å, respectively, indicating single-bond character;[11] this result is in good agreement with the nonaromatic character of the BC_5 rings suggested by NICS calculation (NICS(0) = 5.9), performed at the B3LYP/6-311+G(d,p) level based on the optimized structures at the B3LYP/6-31G(d) level.

Table 1 summarizes the photophysical properties of B-doped PAH **3** and **4**. In toluene, **3** and **4** exhibited strong absorption bands (ε = 23 100 and 19 850) with maximum (λ_{abs}) values at 466 and 495 nm, respectively, attributed to the HOMO−LUMO transition by TD-DFT calculation, performed at the B3LYP/6-311+G(d,p) level based on the optimized structures at the B3LYP/6-31G(d) level. Interestingly, **3** and **4** exhibited strong green fluorescence at 491 and 516 nm with PL quantum yields of 90% and 79%, respectively.[12] The significant red shift in **4** is attributed to the efficient hyperconjugation between the aromatic π orbitals and the aliphatic σ orbitals. The radiative rate constant of **4** was comparable to that of **3** ($k_r = 1.43 \times 10^8$ vs 1.49×10^8 s^{-1}, respectively); however, the nonradiative rate constant of **4** was less than that of **3** ($k_{nr} = 1.6 \times 10^9$ vs 4.0×10^9 s^{-1}, respectively), indicating that the structural flexibility of the substituents accelerates nonradiative decay.

DOI: 10.1021/acs.orglett.5b03167
Org. Lett. 2015, 17, 6158−6161

Table 1. Photophysical Data for 3 and 4[a]

	λ_{ab}[b] (nm)	ε (M^{-1} cm^{-1})	λ_{em}[c] (nm)	Φ_F[d]	τ_F[e] (ns)	k_r/k_{nr}[f] (10^8 s^{-1})
3	466	23 100	491	0.90	6.31	1.43/0.16
4	495	19 850	516	0.79	5.28	1.49/0.40

[a]UV−vis absorption and fluorescence spectra were measured in toluene (2.0×10^{-2} mM). [b]Only the longest absorption maximum was indicated for each compound. [c]Emission maxima upon excitation at 340 nm. [d]Absolute fluorescence quantum yields determined by a calibrated integrating sphere system with ≤3% error. [e]Fluorescence lifetime measured at an emission maxima on excitation at 340 nm. [f]The radiative and nonradiative rate constant (k_r and k_{nr}) were calculated from Φ_F and τ_F using the formula $k_r = \Phi_F/\tau_F$ and $k_{nr} = (1 - \Phi_F)/\tau_F$, respectively.

The redox potential of **3** was measured in CH_3CN by CV: a reversible reduction wave with a peak potential at −1.76 V (vs ferrocene/ferrocenium) was observed. On the other hand, an irreversible oxidation wave was observed; thus, its potential as determined by differential pulse voltammetry (DPV) is 0.92 V.[13] To obtain further information, we prepared a film of **3** by vacuum deposition under a pressure of 5.0×10^{-3} Pa. The ionization potential (I_p) of the film was determined by photoelectron spectroscopy in air to be 5.36 eV, comparable to that estimated from its oxidation potential determined by DPV (5.72 V). Similarly, the electron affinity (E_a = 2.97 V), estimated from I_p and the optical band gap (E_g = 2.39 V), was comparable to that estimated from its oxidation potential determined by CV (3.04 V). Notably, **4** exhibited an I_p (5.20 eV) slightly smaller than that of **3** because of the electron-donating property of the substituents.

For the optimum use of the fluorescent B-doped PAHs, an OLED employing **3** as an emitter was fabricated with the following structure: indium tin oxide (ITO, 150 nm); dipyrazino[2,3-*f*:2′,3′-*h*]quinoxaline-2,3,6,7,10,11-hexacarbonitrile (HAT-CN, 10 nm); *N*,*N*′-di-(1-naphthyl)-*N*,*N*′-diphenyl-(1,1′-biphenyl)-4,4′-diamine (NPD, 60 nm); 5 wt % of **3** and 95 wt % of 9,10-di(2-naphthyl)anthracene (ADN, 20 nm); 1,3,5-tris(1-phenyl-1*H*-benzo[*d*]imidazol-2-yl)benzene (TPBi, 30 nm); LiF (1 nm); Al (100 nm). As shown in Table 2, the device exhibited a green electroluminescence with the Commission Internationale d'Eclairage coordinates of (0.25, 0.60), as well as a promising performance with respect to the driving voltage and luminous efficiencies.[14]

Table 2. Properties of OLED Employing 3 as an Emitter[a]

V_{on} (V)	λ_{max} (nm)	η_c (cd A^{-1})	η_p (lm W^{1-})	η_{ext} (%)	L_{max} (cd m^{-2})
3.5	506	8.7	7.2	2.7	13420

[a]Abbreviations: V_{on}, voltage required for 1 cd m^{-2}; λ_{max}, emission maxima; η_c, maximum current efficiency; η_p, maximum power efficiency; η_{ext}, maximum external quantum efficiency; L_{max}, maximum luminance.

To demonstrate the potential of B-doped PAHs as a semiconducting material, an FET with bottom-gate top-contact configuration was fabricated. The semiconductor film was prepared by spin-coating a chloroform solution of **3**. Figure 3 shows the transfer and output curves, indicating p-type modulation. The hole mobility, threshold voltage, and on−off ratio estimated from the saturation regime were 2.0×10^{-4} cm^2 V^{-1} s^{-1}, − 29.1 V, and 2×10^3, respectively.

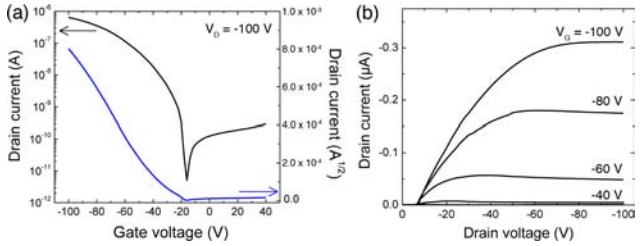

Figure 3. (a) Output and (b) transfer characteristics of an FET device using a spin-coated film of **3** on a Si/SiO_2 substrate.

In summary, tandem intramolecular electrophilic arene borylation was developed for providing facile access to B-doped PAHs. This simple, practical strategy was advantageous for the further extension of π-conjugated frameworks and the introduction of multiple boron atoms, which may spur a bottom-up approach to boron-doped nanocarbons. DFT calculations revealed that electrophilic arene borylation occurred via a four-membered ring transition state, in which C−B and H−Br bonds formed in a concerted manner. Moreover, an organic light-emitting diode and a field-effect transistor were fabricated to demonstrate the promising applications as emitting and semiconducting materials.

■ ASSOCIATED CONTENT

Supporting Information

The Supporting Information is available free of charge on the ACS Publications website at DOI: 10.1021/acs.orglett.5b03167.

Synthesis, analytical data, NMR spectra, DFT studies, CV and DPV measurements, photoelectron spectroscopy, X-ray crystallography, fabrication of OLED and FET (PDF)

Crystallographic data for **3** (CIF)

■ AUTHOR INFORMATION

Corresponding Authors

*E-mail: hatake@kwansei.ac.jp.

*E-mail: nakayama@yz.yamagata-u.ac.jp.

Notes

The authors declare no competing financial interest.

■ ACKNOWLEDGMENTS

This study was supported by a Grant-in-Aid for Scientific Research on Innovative Areas "π-System Figuration: Control of Electron and Structural Dynamism for Innovative Functions" (15H01004) and a Grant-in-Aid for Scientific Research (26288095) from the Ministry of Education, Culture, Sports, Science & Technology in Japan (MEXT) and the MEXT program "Strategic Research Foundation at Private Universities" (S1311046). The authors would like to thank Drs. Tomohiro Ago and Yoshiyuki Mizuhata (Kyoto University) for their support for X-ray crystallography as well as Mrs. Shintaro Nomura and Toshiaki Ikuta (JNC Petrochemical Corporation) for OLED fabrication. The synchrotron X-ray diffraction measurement was performed at the BL38B1 in the SPring-8 by the approval of JASRI (2012A1285, 2012B1194, 2013A1183, 2013B1083).

DOI: 10.1021/acs.orglett.5b03167
Org. Lett. 2015, 17, 6158−6161

REFERENCES

(1) (a) Wu, Z.-S.; Ren, W.; Xu, L.; Li, F.; Cheng, H.-M. *ACS Nano* **2011**, *5*, 5463. (b) Yang, Z.; Yao, Z.; Li, G.; Fang, G.; Nie, H.; Liu, Z.; Zhou, X.; Chen, X.; Huang, S. *ACS Nano* **2012**, *6*, 205. (c) Velez-Fort, E.; Mathieu, C.; Pallecchi, E.; Pigneur, M.; Silly, M. G.; Belkhou, R.; Marangolo, M.; Shukla, A.; Sirotti, F.; Ouerghi, A. *ACS Nano* **2012**, *6*, 10893. (d) Poh, H. L.; Simek, P.; Sofer, Z.; Pumera, M. *ACS Nano* **2013**, *7*, 5262. (e) Wang, L.; Ambrosi, A.; Pumera, M. *Angew. Chem., Int. Ed.* **2013**, *52*, 13818.

(2) (a) Qu, L.; Liu, Y.; Baek, J.-B.; Dai, L. *ACS Nano* **2010**, *4*, 1321. (b) Reddy, A. L. M.; Srivastava, A.; Gowda, S. R.; Gullapalli, H.; Dubey, M.; Ajayan, P. M. *ACS Nano* **2010**, *4*, 6337. (c) Jin, Z.; Yao, J.; Kittrell, C.; Tour, J. M. *ACS Nano* **2011**, *5*, 4112. (d) Ito, Y.; Christodoulou, C.; Nardi, M. V.; Koch, N.; Sachdev, H.; Müllen, K. *ACS Nano* **2014**, *8*, 3337. (e) Zhang, J.; Li, J.; Wang, Z.; Wang, X.; Feng, W.; Zheng, W.; Cao, W.; Hu, P. *Chem. Mater.* **2014**, *26*, 2460.

(3) (a) Otero, G.; Biddau, G.; Sánchez-Sánchez, C.; Caillard, R.; López, M. F.; Rogero, C.; Palomares, F. J.; Cabello, N.; Basanta, M. A.; Ortega, J.; Méndez, J.; Echavarren, A. M.; Pérez, R.; Gómez-Lor, B.; Martín-Gago, J. A. *Nature* **2008**, *454*, 865. (b) Cai, J.; Ruffieux, P.; Jaafar, R.; Bieri, M.; Braun, T.; Blankenburg, S.; Muoth, M.; Seitsonen, A. P.; Saleh, M.; Feng, X.; Müllen, K.; Fasel, R. *Nature* **2010**, *466*, 470. (c) Cloke, R. R.; Marangoni, T.; Nguyen, G. D.; Joshi, T.; Rizzo, D. J.; Bronner, C.; Cao, T.; Louie, S. G.; Crommie, M. F.; Fischer, F. R. *J. Am. Chem. Soc.* **2015**, *137*, 8872. (d) Kawai, S.; Saito, S.; Osumi, S.; Yamaguchi, S.; Foster, A. S.; Spijker, P.; Meyer, E. *Nat. Commun.* **2015**, DOI: 10.1038/ncomms9098.

(4) (a) Fort, E. H.; Scott, L. T. *Angew. Chem., Int. Ed.* **2010**, *49*, 6626. (b) Fort, E. H.; Scott, L. T. *J. Mater. Chem.* **2011**, *21*, 1373. (c) Smalley, R. E.; Li, Y.; Moore, V. C.; Price, B. K.; Colorado, R., Jr.; Schmidt, H. K.; Hauge, R. H.; Barron, A. R.; Tour, J. M. *J. Am. Chem. Soc.* **2006**, *128*, 15824. (d) Yu, X.; Zhang, J.; Choi, W.; Choi, J.-Y.; Kim, J. M.; Gan, L.; Liu, Z. *Nano Lett.* **2010**, *10*, 3343. (e) Dunk, P. W.; Kaiser, N. K.; Hendrickson, C. L.; Quinn, J. P.; Ewels, C. P.; Nakanishi, Y.; Sasaki, Y.; Shinohara, H.; Marshall, A. G.; Kroto, H. W. *Nat. Commun.* **2012**, *3*, 855. (f) Fujihara, M.; Miyata, Y.; Kitaura, R.; Nishimura, Y.; Camacho, C.; Irle, S.; Iizumi, Y.; Okazaki, T.; Shinohara, H. *J. Phys. Chem. C* **2012**, *116*, 15141. (g) Omachi, H.; Nakayama, T.; Takahashi, E.; Segawa, Y.; Itami, K. *Nat. Chem.* **2013**, *5*, 572.

(5) (a) Wu, D.; Zhi, L.; Bodwell, G. J.; Cui, G.; Tsao, N.; Müllen, K. *Angew. Chem., Int. Ed.* **2007**, *46*, 5417. (b) Takase, M.; Enkelmann, V.; Sebastiani, D.; Baumgarten, M.; Müllen, K. *Angew. Chem., Int. Ed.* **2007**, *46*, 5524. (c) Bouit, P.-A.; Escande, A.; Szűcs, R.; Szieberth, D.; Lescop, C.; Nyulászi, L.; Hissler, M.; Réau, R. *J. Am. Chem. Soc.* **2012**, *134*, 6524. (d) Saito, S.; Matsuo, K.; Yamaguchi, S. *J. Am. Chem. Soc.* **2012**, *134*, 9130. (e) Dou, C.; Saito, S.; Matsuo, K.; Hisaki, I.; Yamaguchi, S. *Angew. Chem., Int. Ed.* **2012**, *51*, 12206. (f) Chen, L.; Puniredd, S. R.; Tan, Y.-Z.; Baumgarten, M.; Zschieschang, U.; Enkelmann, V.; Pisula, W.; Feng, X.; Klauk, H.; Müllen, K. *J. Am. Chem. Soc.* **2012**, *134*, 17869. (g) Matsuo, K.; Saito, S.; Yamaguchi, S. *J. Am. Chem. Soc.* **2014**, *136*, 12580. (h) Krieg, M.; Reicherter, F.; Haiss, P.; Ströbele, M.; Eichele, K.; Treanor, M.-J.; Schaub, R.; Bettinger, H. F. *Angew. Chem., Int. Ed.* **2015**, *54*, 8284. (i) Hertz, V. M.; Lerner, H.-W.; Wagner, M. *Org. Lett.* **2015**, *17*, 5240. (j) Hertz, V. M.; Bolte, M.; Lerner, H.-W.; Wagner, M. *Angew. Chem., Int. Ed.* **2015**, *54*, 8800. (k) Osumi, S.; Saito, S.; Dou, C.; Matsuo, K.; Kume, K.; Yoshikawa, H.; Yamaguchi, S. *Chem. Sci.* **2016**, DOI: 10.1039/C5SC02246K. Recent review: (l) Narita, A.; Wang, X.-Y.; Feng, X.; Müllen, K. *Chem. Soc. Rev.* **2015**, *44*, 6616.

(6) (a) Genaev, A. M.; Nagy, S. M.; Salnikov, G. E.; Shubin, V. G. *Chem. Commun.* **2000**, 1587. (b) De Vries, T. S. D.; Prokofjevs, A.; Harvey, J. N.; Vedejs, E. *J. Am. Chem. Soc.* **2009**, *131*, 14679. (c) Hatakeyama, T.; Hashimoto, S.; Seki, S.; Nakamura, M. *J. Am. Chem. Soc.* **2011**, *133*, 18614. (d) Hatakeyama, T.; Hashimoto, S.; Oba, T.; Nakamura, M. *J. Am. Chem. Soc.* **2012**, *134*, 19600. (e) Wang, X.-Y.; Lin, H.-R.; Lei, T.; Yang, D.-C.; Zhuang, F.-D.; Wang, J.-Y.; Yuan, S.-C.; Pei, J. *Angew. Chem., Int. Ed.* **2013**, *52*, 3117. (f) Wang, X.-Y.; Zhuang, F.-D.; Wang, R.-B.; Wang, X.-C.; Cao, X.-Y.; Wang, J.-Y.; Pei, J. *J. Am. Chem. Soc.* **2014**, *136*, 3764. (g) Hirai, H.; Nakajima, K.; Nakatsuka, S.; Shiren, K.; Ni, J.; Nomura, S.; Ikuta, T.; Hatakeyama, T. *Angew. Chem., Int. Ed.* **2015**, *54*, 13581.

(7) Recent reviews: (a) Gather, M. C.; Köhnen, A.; Meerholz, K. *Adv. Mater.* **2011**, *23*, 233. (b) Hofmann, S.; Thomschke, M.; Lüssem, B.; Leo, K. *Opt. Express* **2011**, *19*, A1250. (c) Duan, L.; Qiao, J.; Sun, Y.; Qiu, Y. *Adv. Mater.* **2011**, *23*, 1137. (d) Huang, J.; Su, J.-H.; Tian, H. *J. Mater. Chem.* **2012**, *22*, 10977. (e) Chen, Y.; Ma, D. *J. Mater. Chem.* **2012**, *22*, 18718.

(8) Recent reviews: (a) Gelinck, G.; Heremans, P.; Nomoto, K.; Anthopoulos, T. D. *Adv. Mater.* **2010**, *22*, 3778. (b) Wang, C.; Dong, H.; Hu, W.; Liu, Y.; Zhu, D. *Chem. Rev.* **2012**, *112*, 2208. (c) Sirringhaus, H. *Adv. Mater.* **2014**, *26*, 1319.

(9) (a) Du, C.-J. F.; Hart, H.; Ng, K.-K. D. *J. Org. Chem.* **1986**, *51*, 3162. (b) Saednya, A.; Hart, H. *Synthesis* **1996**, *1996*, 1455. (c) Hatakeyama, T.; Hashimoto, S.; Nakamura, M. *Org. Lett.* **2011**, *13*, 2130.

(10) Schickedanz, K.; Trageser, T.; Bolte, M.; Lerner, H.-W.; Wagner, M. *Chem. Commun.* **2015**, *51*, 15808.

(11) The C−B single bond length is approximately 1.57−1.59 Å. (a) Zettler, F.; Hausen, H. D.; Hess, H. *J. Organomet. Chem.* **1974**, *72*, 157. (b) Olmstead, M. M.; Power, P. P. *J. Am. Chem. Soc.* **1986**, *108*, 4235.

(12) The values for **3** are comparable to those in cyclohexane reported in ref 10: λ_{ab} = 462 nm, λ_{em} = 485 nm, Φ_F = 81%.

(13) The values are comparable to those in *o*-dichlorobenzene reported in ref 10: $E_{1/2}$ = −1.76 V, E_{pa} = 1.14 V.

(14) OLED employing oxa- and azaborine derivatives: (a) Wang, X.; Zhang, F.; Liu, J.; Tang, R.; Fu, Y.; Wu, D.; Xu, Q.; Zhuang, X.; He, G.; Feng, X. *Org. Lett.* **2013**, *15*, 5714. (b) Hashimoto, S.; Ikuta, T.; Shiren, K.; Nakatsuka, S.; Ni, J.; Nakamura, M.; Hatakeyama, T. *Chem. Mater.* **2014**, *26*, 6265. (c) Numata, M.; Yasuda, T.; Adachi, C. *Chem. Commun.* **2015**, *51*, 9443. See also ref 6g.

DOI: 10.1021/acs.orglett.5b03167
Org. Lett. 2015, 17, 6158−6161